# Structure, Function, and Activator-Induced Conformations of the CRSP Coactivator

Dylan J. Taatjes,[1] Anders M. Näär,[1] Frank Andel III,[1,2] Eva Nogales,[1,2] Robert Tjian[1]*

**The human cofactor complexes ARC (activator-recruited cofactor) and CRSP (cofactor required for Sp1 activation) mediate activator-dependent transcription in vitro. Although these complexes share several common subunits, their structural and functional relationships remain unknown. Here, we report that affinity-purified ARC consists of two distinct multisubunit complexes: a larger complex, denoted ARC-L, and a smaller coactivator, CRSP. Reconstituted in vitro transcription with biochemically separated ARC-L and CRSP reveals differential cofactor functions. The ARC-L complex is transcriptionally inactive, whereas the CRSP complex is highly active. Structural determination by electron microscopy (EM) and three-dimensional reconstruction indicate substantial differences in size and shape between ARC-L and CRSP. Moreover, EM analysis of independently derived CRSP complexes reveals distinct conformations induced by different activators. These results suggest that CRSP may potentiate transcription via specific activator-induced conformational changes.**

Initiation of eukaryotic transcription is regulated at multiple stages by mechanisms involving activators, core promoter recognition complexes, and chromatin modifying factors (*1, 2*). Once assembled at their cognate DNA sites, sequence-specific enhancer binding proteins typically rely upon various types of coactivators to communicate activation signals to the preinitiation complex, which consists of transcription factors IIA (TFIIA), TFIIB, TFIID, TFIIE, TFIIF, TFIIH, and RNA polymerase II. One large class of eukaryotic transcriptional coactivators is characterized by the ability to potentiate transcription via interactions with activators and/or the basal transcription apparatus. Among this diverse group of transcriptional cofactors are multisubunit complexes such as yeast Mediator, as well as a cadre of related metazoan coactivators, which include the ARC/DRIP, TRAP/SMCC, hMed, NAT, CRSP, and PC2 complexes (*3–11*). These metazoan complexes contain a few subunit homologs of yeast Mediator proteins, whereas the majority of their subunits appear to have diverged considerably, likely reflecting the greater complexity of metazoan gene regulatory pathways.

The various mammalian cofactor complexes can be grouped into two general categories consisting of a set of larger (ARC/DRIP, TRAP/SMCC, hMed, and NAT) and smaller (CRSP and PC2) cofactors. Whereas these "large" and "small" cofactors share many subunits, the larger complexes contain additional polypeptides (ARC240, ARC250, cdk8, and cyclin C) not present in the smaller CRSP and PC2 complexes. This distinguishing structural feature has not been clearly linked to distinct functional characteristics. In fact, both cofactor subclasses (large and small) generally display coactivator function in in vitro transcription assays, although NAT and SMCC may mediate a form of repression (*3–5, 7–11*). Here, we present evidence that correlates distinguishing structural features with transcriptional function in the context of the ARC (large) and CRSP (small) cofactors. In addition, our structural analysis indicates that an aspect of coactivator (CRSP) function may involve specific activator-induced conformational changes.

We initiated EM structural studies on an ARC cofactor fraction purified from HeLa nuclear extract as described previously (*8*). A phosphocellulose 1.0 M KCl eluate was used to isolate ARC via a VP16 affinity resin (*8*); the eluted ARC sample was then applied to a glycerol gradient. Subsequent classification of ARC particle images in electron micrographs of negatively stained samples showed that the affinity-purified ARC preparation contained two complexes of distinct size and shape, present in approximately a 60:40 ratio (small:large; Fig. 1A). Similar results were obtained using ARC complexes isolated via an SREBP-1a (*8*) affinity resin (*12*). To better separate the two complexes, the affinity-purified ARC sample was subjected to "higher-resolution" glycerol gradient sedimentation in which the sample represented <5% of the total gradient volume. This typically sedimented the small complex in fraction 13, whereas the large complex was concentrated in fraction 17. SDS–polyacrylamide gel electrophoresis (SDS-PAGE) (Fig. 1B) and western blot analysis (*12*) confirmed that the small complex was highly related (or identical) to the previously identified CRSP coactivator (*10*), whereas the large complex possessed a subunit composition characteristic of the ARC/DRIP and TRAP/SMCC complexes (*4, 5, 8, 9*). Thus, previous ARC preparations (*8*) most likely contained two distinct, structurally stable complexes. We will provisionally refer to the large complex as ARC-L (ARC-Large) and the small complex as CRSP. The "CRSP" designation is based primarily on the presence of CRSP70, which appears to be CRSP-specific (see below).

We next determined whether the differences in complex structure and subunit composition might reflect different transcriptional cofactor properties. For this functional analysis, we used an in vitro–reconstituted transcription system (*13*) comprising an LDLR-derived template assembled into chromatin by the S-190 system (*14*). This chromatin template was then used to direct Sp1/SREBP-dependent activation of transcription in a reaction containing purified and recombinant human transcription factors (TFIIA, TFIIB, TFIID, TFIIE, TFIIH, TFIIF, and RNA polymerase II). When we tested the activity of glycerol gradient fractions containing CRSP, but little or no ARC-L, we observed robust Sp1/SREBP-dependent activation (Fig. 2A, lanes 7 and 8). Analysis of samples containing a mixture of CRSP and ARC-L revealed that as the ratio of ARC-L/CRSP increased, there was a concomitant decrease in transcriptional activity (Fig. 2A, lanes 10, 12, and 14). Note, however, that some activation still occurred at the higher ARC-L ratio (lane 14). This was because glycerol gradient purification, although effective in yielding CRSP fractions largely free of ARC-L, was not able to generate ARC-L fractions completely free of CRSP (gradient fractions most concentrated in ARC-L still contained ~30 to 40% CRSP, based on statistical analysis of EM data). Therefore, to obtain an ARC-L sample devoid of CRSP, we immunodepleted these fractions with an antibody to CRSP70 (anti-CRSP70), which recognizes only the CRSP complex [see supplementary information (*15*)]. When CRSP was immunodepleted from these ARC-L fractions, there was a

[1]Howard Hughes Medical Institute and [2]Lawrence Berkeley National Laboratory, Department of Molecular and Cell Biology, 401 Barker Hall, University of California, Berkeley, CA 94720, USA.

*To whom correspondence should be addressed. E-mail: jmlim@uclink4.berkeley.edu

dramatic loss of coactivator activity (Fig. 2A, lane 16), indicating that highly purified ARC-L is unable to potentiate transcriptional activity in this assay. By contrast, when glycerol gradient fractions were exhaustively depleted of ARC-L by anti-cdk8 immunodepletion, there was no detectable decrease in transcriptional activity (Fig. 2A, compare lanes 6 and 8), consistent with our previously reported findings (*8*). As an additional control, we isolated CRSP by an entirely independent method using an anti-Flag resin to immunopurify the CRSP complex from a cell line expressing Flag-tagged CRSP70 (*16*). This "Flag-CRSP" complex (eluted with Flag peptide) also strongly potentiated activator-dependent transcription (Fig. 2A, lane 4). The CRSP complex isolated via Flag-CRSP70 immunopurification exhibited a subunit composition that was indistinguishable from glycerol gradient affinity-purified CRSP as determined by immunoblot and silver stain analysis (*12*).

To further confirm these findings, we immunopurified CRSP and ARC-L from the P1M fraction using antibodies directed against CRSP70 and cdk8. Each separate immunoprecipitated complex was tested for transcriptional activity by supplementing the reconstituted transcription reaction with cofactor-bound affinity beads. Activator-dependent transcription was observed for the CRSP70 immunoprecipitated complex (Fig. 2B, lanes 3 and 4); in contrast, resins containing only the ARC-L complex (α-cdk8) were essentially inactive (Fig. 2B, lanes 1 and 2). A "beads only" mock immunoprecipitate was used as a negative control (Fig. 2B, lanes 5 and 6) and showed no activity. These functional assays indicate that the ARC250, ARC240, cdk8, and cyclin C subunits present in ARC-L may somehow render the complex inactive, at least in this LDLR-derived promoter context.

Structural analyses were performed with the same ARC-L and CRSP samples used for the functional assays. Samples were analyzed in negative stain (uranyl acetate) using EM and single-particle image reconstruction techniques. Further details regarding image processing are provided as supplementary information (*15*). The three-dimensional (3D) structure of ARC-L is shown in Fig. 3A. Defined "body," "leg," and "foot" regions are clearly distinguishable and are consistent with the structural features of the TRAP complex, which has similar subunit composition (*17*). The leg contacts the foot at one point and the body at two sites, giving rise to a hole halfway along the length of the cofactor. The foot region is oriented at a right angle to the body, giving the complex an "L" shape as shown by the side (orientation 3) view of the complex in Fig. 3A.

Structural studies of CRSP were initiated using a VP16 affinity-purified sample. The VP16-CRSP structure possesses three distinct regions, including a hook-like "leg" domain and a central "body" connected by two contacts to a "head" region (Fig. 3B). The complex is quite elongated and narrow (360 Å by 145 Å) and contains holes at each end. Comparison of the VP16-CRSP structure with ARC-L (also isolated via VP16) reveals important structural relationships. A superposition of the complexes, on the basis of their related struc-

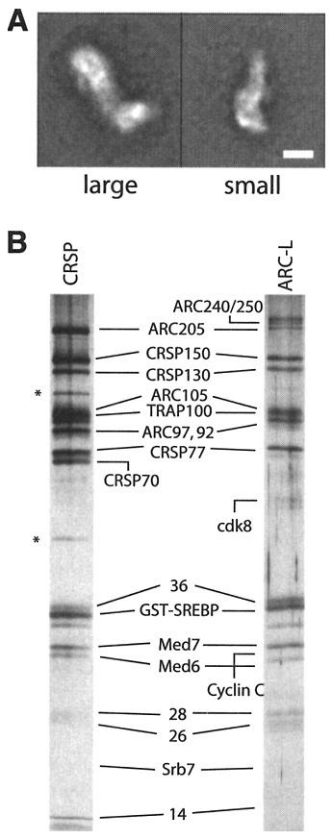


**Fig. 1.** Activators bind two distinct cofactor complexes. (**A**) Structural separation of the complexes by image processing. VP16 affinity-purified "ARC" was analyzed by EM. A total of 2027 particles and their corresponding tilt pairs were windowed, aligned, and merged into 26 classes. Two-dimensional averages representing two of these classes are shown, indicative of the different-sized complexes observed in the affinity-purified ARC sample (bar, 150 Å). (**B**) Subunit compositions of small (CRSP) and large (ARC-L) complexes. SDS-PAGE (5 to 15%) silver stain analysis indicates presence of CRSP70 specifically in CRSP and ARC240, ARC250, cdk8, and cyclin C specifically in ARC-L. Presence (or lack) of many subunits have been corroborated by western blot (*12*). Asterisks denote nonspecific bands that do not consistently copurify with the CRSP complex. Data shown utilized an SREBP-1a affinity-purification step. Analogous results were obtained using VP16 affinity-purification.

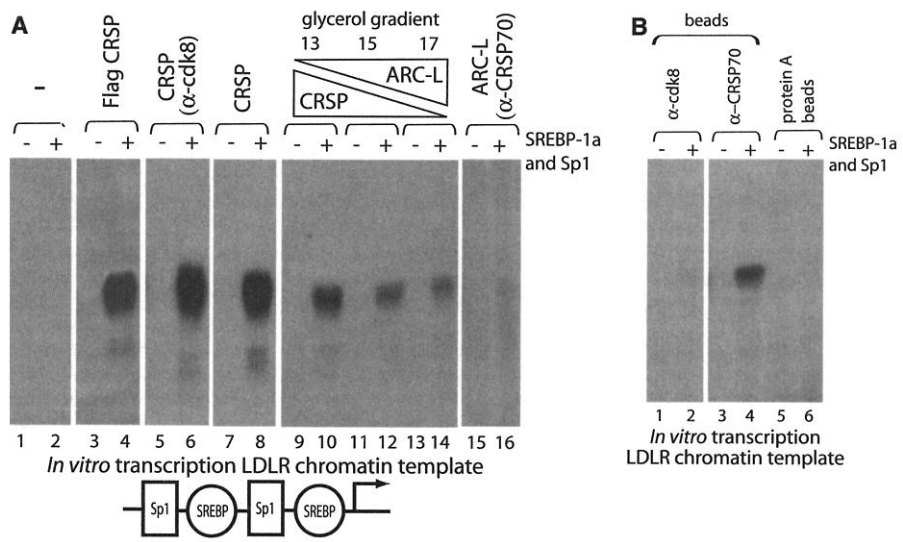


**Fig. 2.** CRSP and ARC-L have contrasting transcriptional cofactor properties. (**A**) In vitro transcription analysis of ARC-L and CRSP on an LDLR-derived chromatin template. Transcription reactions were performed in the presence (+) and absence (–) of SREBP-1a (5 nM) and Sp1 (2 nM). Reactions were supplemented with CRSP and ARC-L as shown. Lanes 1 and 2: no cofactor added. Lanes 3 and 4: CRSP isolated via Flag-tagged CRSP70 (peptide eluted). Lanes 5 and 6: affinity-purified (SREBP) CRSP immunodepleted of ARC-L via α-cdk8. Lanes 7 and 8: affinity-purified (SREBP) CRSP. Lanes 9 through 14: affinity-purified (VP16) samples containing mixtures of CRSP and ARC-L. Lanes 15 and 16: affinity-purified (VP16) ARC-L immunodepleted of CRSP via α-CRSP70. Equal amounts of cofactor(s) were added to each transcription reaction on the basis of silver stain analysis (*12*). (**B**) In vitro transcription reactions of immunoprecipitated complexes. Reactions were executed as in (A), except that added cofactor complexes were bound to protein A beads via the antibody indicated. Equal amounts of the immunoprecipitated complexes were added to each transcription reaction on the basis of silver stain analysis (*12*).

tural features, is depicted in Fig. 3C. Both possess similar head/body and leg regions; in fact, the shape and location of the hole in the leg region of VP16-CRSP and (VP16) ARC-L is virtually identical. However, the CRSP complex apparently lacks some protein density in its head/body region and is completely devoid of the foot domain present in ARC-L. This is highlighted by the corresponding difference map (ARC-L minus CRSP) shown in Fig. 3D. Figure 3E shows the location of the VP16 activator binding site on the CRSP complex, on the basis of EM analysis and difference mapping of VP16-CRSP samples following incubation with anti-GST [VP16 affinity purification utilizes a glutathione *S*-transferase (GST) fusion protein]. EM samples of VP16-CRSP were prepared as described above, followed by addition of the antibody (in a fivefold excess). Two independent experiments were run: one with a polyclonal and one with a monoclonal antibody to GST. Both experiments yielded the same result. Note that the location of the VP16 binding site is exposed in both the CRSP and ARC-L complexes.

Because Flag-CRSP was essentially identical in function and subunit composition (Fig. 2) (*12*) relative to VP16-CRSP, we presumed that these independently purified complexes would possess similar structural characteristics. However, EM analysis revealed that the Flag-CRSP complex adopted a different conformation (compare Fig. 4A and 4B). Although it retained distinct head, body, and leg domains, the overall shape of the "activator-free" Flag-CRSP structure was wider (180 Å versus 145 Å), shorter (300 Å versus 360 Å), and flatter (130 Å versus 150 Å) than the VP16-CRSP structure. Further, it appeared that the second bridge between the head and body region was displaced to a more central location in the Flag-CRSP conformer (Fig. 4, A and B; compare structures in row 1).

Having obtained two quite distinct structures for activator-free (Flag) CRSP versus activator (VP16)–bound CRSP, we next examined the structure of CRSP bound to a different activator, SREBP-1a. EM analysis of SREBP-CRSP revealed a third distinct conformation (Fig. 4C) with few structural similarities to Flag-CRSP and even fewer to VP16-CRSP (compare structures in Fig. 4). Although the length and width (305 Å by 180 Å) of SREBP-CRSP was similar to Flag-CRSP, it possessed greater structural variation in its head and body regions, appearing considerably more hollow in its center. This resulted in the complex being a bit "broader" (165 Å versus 130 Å) (Fig. 4, B and C; compare structures in row 2) with respect to Flag-CRSP. In addition to the qualitative comparisons in Fig. 4, cross-correlation [detailed in supplementary information (*15*)] of the structures demonstrates that VP16-CRSP, Flag-CRSP, and SREBP-CRSP are conformationally distinct. Figure 4D shows the region (highlighted in yellow) likely to contain the SREBP binding site. This site was identified

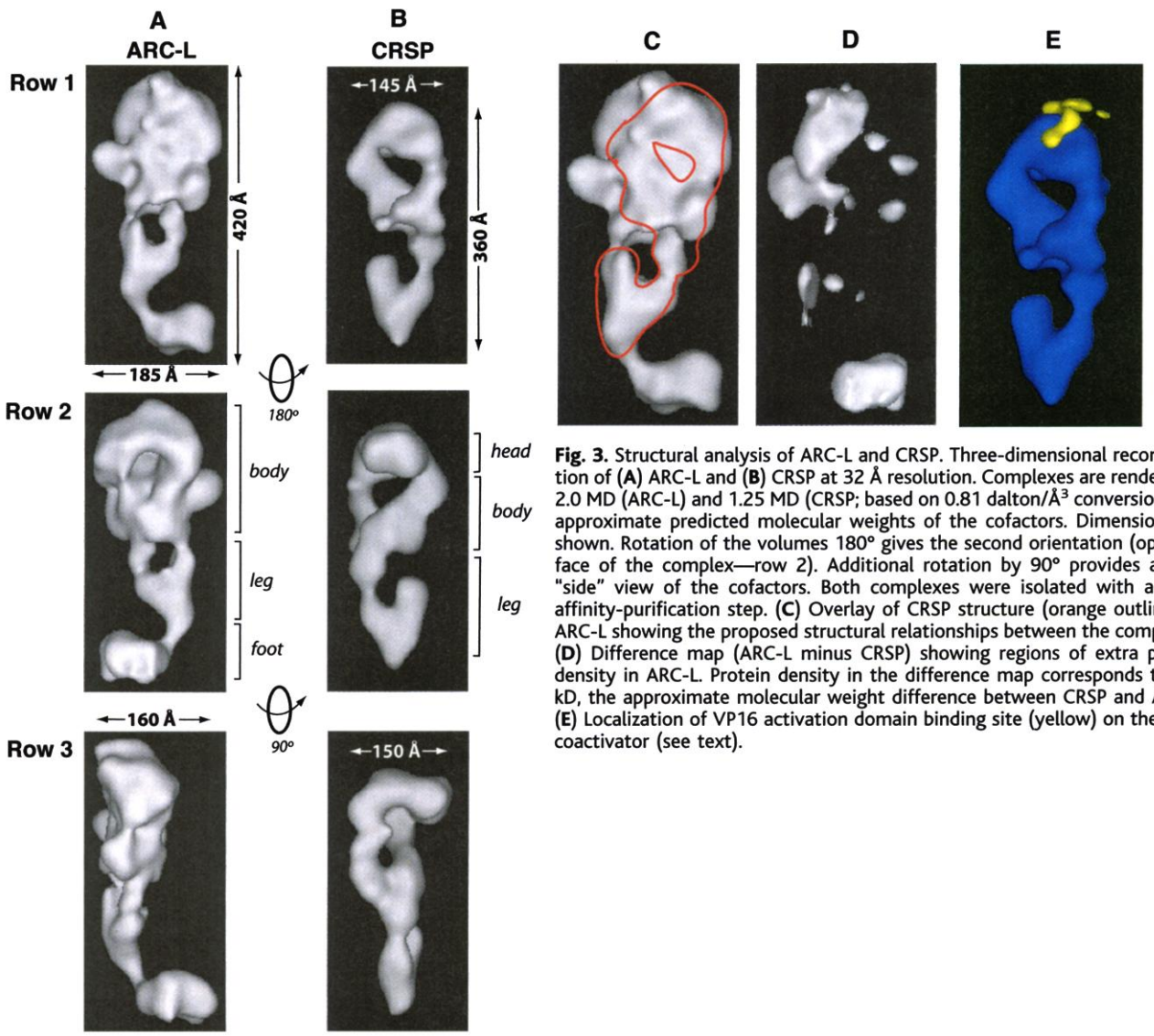


**Fig. 3.** Structural analysis of ARC-L and CRSP. Three-dimensional reconstruction of (**A**) ARC-L and (**B**) CRSP at 32 Å resolution. Complexes are rendered to 2.0 MD (ARC-L) and 1.25 MD (CRSP; based on 0.81 dalton/Å$^3$ conversion), the approximate predicted molecular weights of the cofactors. Dimensions are shown. Rotation of the volumes 180° gives the second orientation (opposite face of the complex—row 2). Additional rotation by 90° provides a third "side" view of the cofactors. Both complexes were isolated with a VP16 affinity-purification step. (**C**) Overlay of CRSP structure (orange outline) on ARC-L showing the proposed structural relationships between the complexes. (**D**) Difference map (ARC-L minus CRSP) showing regions of extra protein density in ARC-L. Protein density in the difference map corresponds to 700 kD, the approximate molecular weight difference between CRSP and ARC-L. (**E**) Localization of VP16 activation domain binding site (yellow) on the CRSP coactivator (see text).

from EM analysis and difference mapping of structures generated by incubation of SREBP-CRSP with anti-GST antibodies, which target the GST–SREBP-1a activator fusion (*8*). As with the VP16 localization experiments (see above), both polyclonal and monoclonal antibodies were used in two independent analyses, both of which generated the same result.

To provide additional evidence for activator-induced structural alterations in CRSP, we selectively converted activator-free Flag-CRSP to either the VP16 or SREBP conformation. This was done by first affinity-purifying Flag-CRSP on an anti-Flag affinity column. Then, either SREBP-1a or VP16 (*8*) was allowed to bind the immobilized Flag-CRSP prior to peptide elution from the anti-Flag affinity resin. Subsequent EM analysis and 3D reconstruction revealed that the predicted activator-induced conformational changes had occurred. The Flag-CRSP sample which bound VP16 structurally resembled the VP16 affinity-purified complex shown in Fig. 4A; similarly, Flag-CRSP which bound SREBP was converted to a conformation that corresponded specifically with Fig. 4C. Cross-correlation analysis further established the integrity of the conformational changes. The 3D structures and correlation analysis of these Flag-converted structures are included with the supplementary information (*15*). As with previous EM analyses, each reconstruction was conducted completely independently for both samples without reference bias. On the basis of the conformational consistency and reproducibility shown by these independent structural comparisons (Fig. 4) (*15*), we conclude that the CRSP coactivator is conformationally flexible and can assume significantly different 3D structures when bound to different activators.

The ARC and CRSP cofactor complexes, originally purified from human cells by independent means, presented a dilemma with regard to their structural and functional relationships. In this study, we used a combination of biochemical separation methods, in vitro transcription assays, and EM-based structural analysis to resolve potential functional and structural differences. These studies reveal three unexpected findings. First, previously defined ARC preparations (*8*) actually consist of two distinct and stable multisubunit complexes, identified as ARC-L and CRSP. Second, functional analyses of the ARC-L and CRSP complexes reveal that the larger ARC-L complex is transcriptionally inactive, whereas the smaller CRSP complex displays potent coactivator function in vitro. Third, and perhaps most surprisingly, EM analysis and 3D reconstruction of CRSP, either not bound to ligand or bound to two different activation domains, reveals three distinct structures. This third finding suggests that CRSP may undergo substantial conformational alterations induced by binding different activators. Such activator-induced structural changes may have a profound impact on the mechanism of transcriptional activation in vivo and highlights the potential importance of coactivator structural plasticity in the formation of transcriptionally active preinitiation complexes.

Although CRSP and ARC-L both bind activators with high affinity, they display contrasting transcriptional properties. This suggests that one mechanism for transcription regulation may involve modulation of transcriptional activity by the ARC-L–specific subunits. The presence of ARC240, ARC250, and cdk8/cyclin C may halt transcription by favoring formation of the inactive ARC-L complex (with concomitant loss of CRSP70), as shown in Fig. 5. Such a model is supported by our in vitro transcription assays; the NAT and SMCC cofactors, which have subunit compositions similar to ARC-L, have also displayed transcriptional inactivity in other in vitro assays (*5, 11*). Given that a prominent difference between ARC-L and CRSP is the presence of ARC240, ARC250, and cdk8/cyclin C, it is likely that these subunits play a negative role in transcriptional regulation. Indeed, cdk8 is known to inhibit RNA polymerase II elongation by blocking TFIIH-mediated phosphorylation of the RNA polymerase CTD (*18*). Conversely, the CRSP70 subunit may play an important role in the coactivator function of the CRSP complex. This is suggested by its conspicuous absence in the inactive ARC-L cofactor. Additionally, CRSP70 contains a region highly homologous to TFIIS, suggesting it may mediate a key interaction with RNA polymerase II (*19*).

EM analysis and 3D reconstruction of ARC-L and CRSP revealed important structural relationships. The extra protein density in ARC-L appears to reside in both the head and the foot domains, suggesting that the additional ARC-L components do not bind as a single "subcomplex." The predicted mass of the foot domain is 330 kD. The combined mass of cdk8/cyclin C is about 90 kD; thus, the foot region of ARC-L most likely contains (at least) one of the ARC240 or ARC250 polypeptides.

Structural analysis of the CRSP coactivator reveals that activator binding induces dramatic structural changes in the complex, which appear to be activator-specific. One reason for the observed activator-specific changes may be that the VP16 and SREBP-1a activation domains target different subunits in the CRSP complex [CRSP77 versus ARC105(TIG-1), respectively] (*20, 21*) and these distinct activator-targeted subunits may act as a "switch" to orchestrate specific conformational changes. The differences in conformation cannot be attributed to the

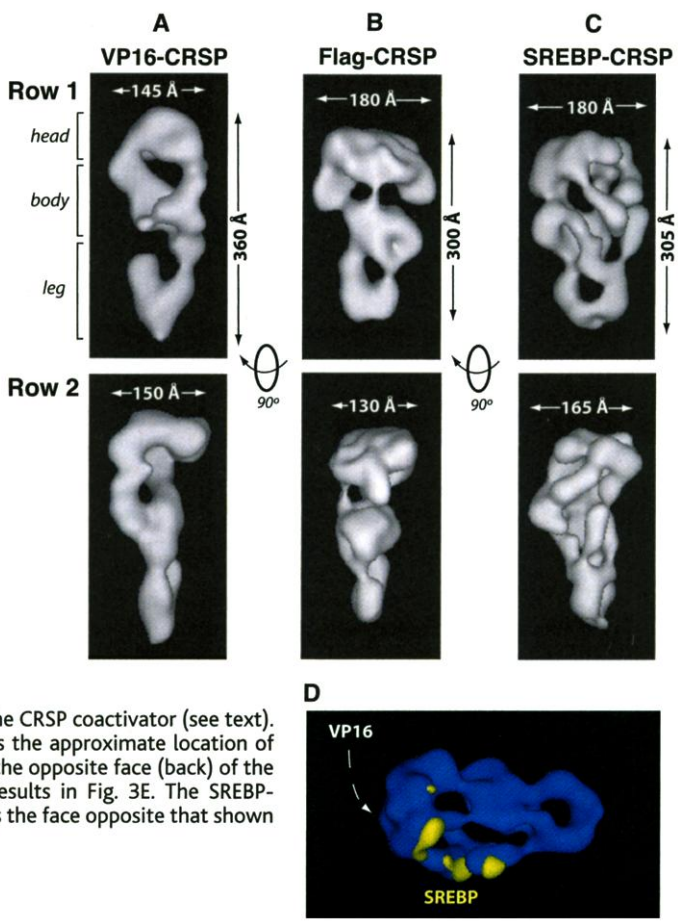


**Fig. 4.** Structures of (**A**) VP16-CRSP, (**B**) Flag-CRSP, and (**C**) SREBP-CRSP show substantial differences in conformation. Each complex is rendered to 1.25 MD, which approximates their predicted molecular masses. Dimensions are as shown; structures have been filtered to 32 Å resolution. Structures across each row (1 and 2) show the same relative orientation. (Note: The relative orientations of the complexes cannot be known with absolute certainty because each structure was generated independently via random conical tilt.) Complexes in row 2 are rotated 90° with respect to row 1, showing the side view of the coactivator. (**D**) Localization of SREBP binding site (yellow) on the CRSP coactivator (see text). The white arrow indicates the approximate location of the VP16 binding site on the opposite face (back) of the complex, based on the results in Fig. 3E. The SREBP-CRSP orientation shown is the face opposite that shown in (C), row 1.

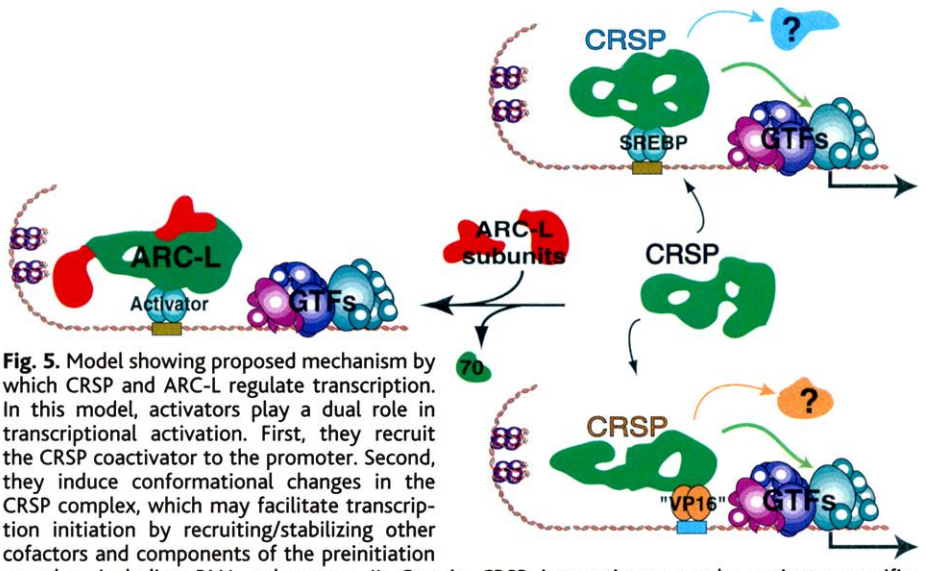


**Fig. 5.** Model showing proposed mechanism by which CRSP and ARC-L regulate transcription. In this model, activators play a dual role in transcriptional activation. First, they recruit the CRSP coactivator to the promoter. Second, they induce conformational changes in the CRSP complex, which may facilitate transcription initiation by recruiting/stabilizing other cofactors and components of the preinitiation complex, including RNA polymerase II. Certain CRSP interactions may be activator-specific. However, upon binding additional ARC-L subunits (which may occur on activator-bound CRSP following multiple rounds of activated transcription), CRSP undergoes a structural change that may also result in dissociation of CRSP70. Now converted to ARC-L, coactivator function is lost and activated transcription is inhibited. The location of ARC-L–specific polypeptides (red) is based upon analysis detailed in Fig. 3D. The orientations of the complexes at the promoter are speculative. VP16 is shown in quotation marks because it does not directly bind DNA.

mere presence of the activation domain because of its small size (about 6% of the total mass) relative to the CRSP complex. Further, we have mapped the VP16 and SREBP-1a binding sites to comparatively small and distinct regions on the CRSP complex. This provides direct evidence that only a limited number (one or perhaps two) of CRSP subunits are targeted by a particular activator. Because VP16-CRSP and SREBP-CRSP are conformationally distinct in regions distal to the activator binding sites, we suggest that activator binding may induce long-range conformational changes. Thus, different protein surfaces in CRSP are likely exposed as a consequence of activator binding.

The conformational flexibility of the CRSP coactivator may have important implications for its mechanism of action. CRSP and its related coactivator complexes appear to be generally required for transcription and are targeted by a diverse array of regulatory proteins (*22*). Interestingly, different transcription activators can target different subunits of the CRSP complex (*3, 9, 20, 21*). Thus, despite binding the same coactivator complex, regulatory proteins may impart promoter-specific functions that may be dependent on CRSP conformation. For example, specific activator-induced CRSP conformations may regulate binding and recruitment of additional activators or cofactors to the preinitiation complex (Fig. 5). Furthermore, these conformational changes may trigger other (as yet undiscovered) enzymatic activities within the CRSP coactivator. Indeed, adopting a number of activator-dependent conformations may enable CRSP to perform more specialized roles in transcriptional activation. Elucidation of these roles will be an important subject of future work.

### References and Notes


1. R. E. Kingston, G. J. Narlikar, *Genes Dev.* **13**, 2339 (1999).
2. B. D. Lemon, R. Tjian, *Genes Dev.* **14**, 2551 (2000).
3. T. G. Boyer, M. E. D. Martin, E. Lees, R. P. Riccardi, A. J. Berk, *Nature* **399**, 276 (1999).
4. J. D. Fondell, H. Ge, R. G. Roeder, *Proc. Natl. Acad. Sci. U.S.A.* **93**, 8329 (1996).
5. W. Gu *et al.*, *Mol. Cell* **3**, 97 (1999).
6. Y. Kim, S. Bjorklund, Y. Li, M. H. Sayre, R. D. Kornberg, *Cell* **77**, 599 (1994).
7. S. Malik, W. Gu, W. Wu, J. Qin, R. G. Roeder, *Mol. Cell* **5**, 753 (2000).
8. A. M. Näär *et al.*, *Nature* **398**, 828 (1999).
9. C. Rachez *et al.*, *Nature* **398**, 824 (1999).
10. S. Ryu, S. Zhou, A. G. Ladurner, R. Tjian, *Nature* **397**, 446 (1999).
11. X. Sun *et al.*, *Mol. Cell* **2**, 213 (1998).
12. D. J. Taatjes, A. M. Näär, R. Tjian, data not shown.
13. A. M. Näär *et al.*, *Genes Dev.* **12**, 3020 (1998).
14. R. T. Kamakaka, M. Bulger, J. T. Kadonaga, *Genes Dev.* **7**, 1779 (1993).
15. Supplementary data is available at *Science* Online at www.sciencemag.org/cgi/content/full/295/5557/1058/DC1
16. The P1M fraction from a stable 293T human kidney cell line expressing Flag-tagged CRSP70 was used for CRSP purification via an anti-Flag affinity resin.
17. M. R. Dotson *et al.*, *Proc. Natl. Acad. Sci. U.S.A.* **97**, 14307 (2000).
18. S. Akoulitchev, S. Chuikov, D. Reinberg, *Nature* **407**, 102 (2000).
19. V. Booth, C. M. Koth, A. M. Edwards, C. H. Arrowsmith, *J. Biol. Chem.* **275**, 31266 (2000).
20. M. Ito *et al.*, *Mol. Cell* **3**, 361 (1999).
21. A. M. Näär, unpublished results.
22. C. Rachez, L. P. Freedman, *Curr. Opin. Cell Biol.* **13**, 274 (2001).



23. We thank J. Berger, J. Doudna, R. Freiman, A. Ladurner, B. Lemon, R. Losick, M. Marr, D. Rio, K. Shelton, and K. Yamamoto for critical reading of the manuscript. We also thank A. Ladurner and S. Ryu for the flag-70 cell line; A. Ladurner, S. Ryu, and W. Zhai for antibodies against CRSP70; Y. Nedialkov and S. Triezenberg for monoclonal antibodies against GST; and O. Fedin for scanning micrographs. D.J.T. is supported by a grant from the American Cancer Society (#PF0007801GMC). This work was funded by grants from the NIH and Howard Hughes Medical Institute.

9 August 2001; accepted 7 December 2001


# Linking Breeding and Wintering Ranges of a Migratory Songbird Using Stable Isotopes


**D. R. Rubenstein,[1,2*†] C. P. Chamberlain,[2‡] R. T. Holmes,[1] M. P. Ayres,[1] J. R. Waldbauer,[2‡] G. R. Graves,[3] N. C. Tuross[4]**



**We used the natural abundance of stable isotopes (carbon and hydrogen) in the feathers of a neotropical migrant songbird to determine where birds from particular breeding areas spend the winter and the extent to which breeding populations mix in winter quarters. We show that most birds wintering on western Caribbean islands come from the northern portion of the species' North American breeding range, whereas those on more easterly islands are primarily from southern breeding areas. Although segregated by breeding latitude, birds within local wintering areas derive from a wide range of breeding longitudes, indicating considerable population mixing with respect to breeding longitude. These results are useful for assessing the effects of wintering habitat loss on breeding population abundances and for predicting whether the demographic consequences will be concentrated or diffuse.**


In recent decades, many species of neotropical migrant birds have shown marked changes in abundance—both increases and decreases—in parts of their North American breeding range (*1*, *2*). These changes may be due to events occurring in the breeding